Volume 18 | Number 18 | 14 May 2016 | Pages 3153–3308

CrystEngComm

www.rsc.org/crystengcomm

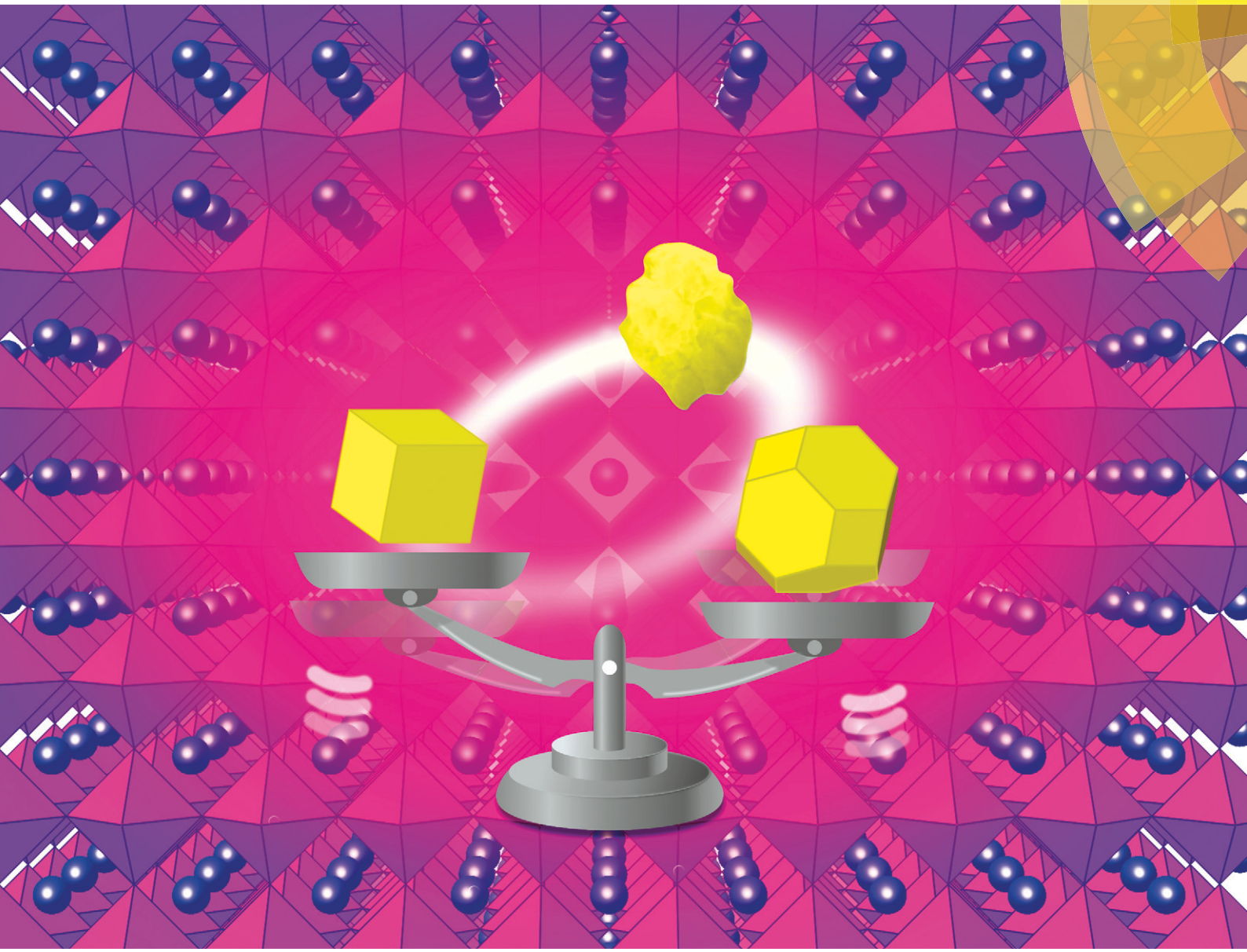

ROYAL SOCIETY OF CHEMISTRY

PAPER

Kazunari Domen *et al.*

Effects of flux treatment on morphology of single-crystalline $BaNbO_2N$ particles

175 YEARS

CrystEngComm

PAPER

View Article Online
View Journal | View Issue

Cite this: *CrystEngComm*, 2016, **18**, 3186

Effects of flux treatment on morphology of single-crystalline $BaNbO_2N$ particles†

Masanori Kodera, Masao Katayama, Takashi Hisatomi, Tsutomu Minegishi and Kazunari Domen*

Received 30th November 2015,
Accepted 18th January 2016

DOI: 10.1039/c5ce02335a

www.rsc.org/crystengcomm

The effect of different kinds of alkali halide flux treatments on the morphology of $BaNbO_2N$ particles was investigated. $BaNbO_2N$ powder was first synthesized by heating a mixture of $BaCO_3$ and Nb_2O_5 under NH_3 flow. Following synthesis, the powder was again heated under NH_3 flow but in the presence of a flux. In the case of a NaCl flux, highly crystalline cubic particles were obtained. On the other hand, a KCl flux led to the formation of truncated octahedral particles. Although particles with clear crystal habits were obtained, it was found that they were actually an aggregation of primary particles, all with the same crystal orientation. A systematic survey of the effect of the different fluxes revealed that the type of cation in the flux played a major role in determining the morphology of the $BaNbO_2N$ particles. It was also revealed that a vaporized flux was also effective in changing the particle morphology.

1. Introduction

Oxynitrides have recently attracted much attention for their various potential applications, such as pigments, dielectrics, and photocatalysts.[1–6] They have been intensively studied as photocatalysts because of their appropriate bandgap energy for absorbing visible light and their suitable band alignment for the water splitting reaction. Among these compounds, there has been a particular interest in perovskite-type oxynitrides, generally denoted as $AB(O,N)_3$.[7,8] $BaNbO_2N$ has a perovskite-type structure and an optical absorption edge at about 740 nm, which is the longest wavelength reported for a transition metal oxynitride.[9,10] In order to achieve high performance as photocatalysts or photoelectrodes, the crystallinity of oxynitrides is one of the most important factors. However, unlike oxide materials, for which several approaches such as hydrothermal synthesis and flux methods can be used to prepare highly crystalline particles,[11–14] for oxynitrides the options are rather limited.

High-quality oxynitride crystals can be prepared using flux synthesis. The flux method can be applied during synthesis of oxide precursors, during nitridation of starting materials or oxide precursors, or during post treatment of oxynitrides. In the first method, a flux is mixed with starting materials such as metal oxides, carbonates and nitrates, which are then heated in air or an inert atmosphere to obtain oxide precursors. Nitridation is then performed to produce the final oxynitrides. Highly crystalline $SrTaO_2N$ and $LaTiO_2N$ have been synthesized using this procedure from $Sr_2Ta_2O_7$ and $La_2Ti_2O_7$, respectively.[15,16] In this situation, the oxide precursors have a similar crystal structure to that of the final oxynitrides. However, one of the difficulties in synthesizing well-crystallized $BaNbO_2N$ is that there is no suitable precursor oxide material with a Ba/Nb ratio of 1. This leads to a large change in the crystal structure during the nitridation process. Another means of applying the flux method to prepare oxynitrides is to mix the flux with the starting materials or oxide precursors, which are then heated under an NH_3 flow to promote crystal growth. Takata *et al.* applied this approach to synthesizing Ta_3N_5,[17] and Kim reported the effects of a KCl flux on $CaTaO_2N$, $SrTaO_2N$ and $LaTaON_2$.[18] These (oxy)nitrides contain Ta atoms. However, if this method is used to synthesize $BaNbO_2N$, it is likely that chemical reduction of Nb species and/or contamination by flux components would occur due to the long reaction time required. The third approach is to apply a flux treatment to an already synthesized oxynitride. The flux is mixed with the oxynitride, which is then heated under an NH_3 flow. This method may be expected to lead to a fairly rapid improvement in crystallinity, because no drastic change in composition or crystal structure occurs. However, there has so far been no report focusing on the application of such a flux treatment to Nb-containing

Department of Chemical System Engineering, School of Engineering, The University of Tokyo, 7-3-1 Hongo, Bunkyo-ku, Tokyo 113-8656, Japan. E-mail: domen@chemsys.t.u-tokyo.ac.jp

† Electronic supplementary information (ESI) available. See DOI: 10.1039/c5ce02335a

oxynitrides. Hence, in the present study, the effect of different post-synthesis flux treatments on the crystallinity and morphology of $BaNbO_2N$ particles was investigated.

2. Experimental

$BaNbO_2N$ particles were prepared by heating a mixture of $BaCO_3$ and Nb_2O_5 under an NH_3 flow. The Ba/Nb ratio in the starting material was adjusted to 1.5 in order to suppress the formation of the NbO_xN_y impurity phase due to volatilization of Ba during the nitridation process.[19] Nitridation was performed at 1173 K for 10 h under an NH_3 flow of 150 mL min^{-1}. After the synthesis of $BaNbO_2N$, different flux treatments were carried out. The $BaNbO_2N$ powder was mixed with either LiCl, NaCl, KCl, RbCl, CsCl, KF, KBr, or KI, and heated at 1173 K for 3 h under an NH_3 flow of 100 mL min^{-1}. The flux/$BaNbO_2N$ molar ratio was fixed at 5 unless otherwise mentioned. After the flux treatment, most of the flux component had evaporated, and the obtained samples were washed with a sufficient amount of distilled water to remove the remained flux. Hereafter, the final flux-treated samples are denoted as $BaNbO_2N$(flux type), *e.g.*, $BaNbO_2N$(NaCl). The crystal structure of the samples was identified using X-ray diffraction (XRD; Rigaku, RINT Ultima III, CuKα source). Ultraviolet-visible (UV-vis) diffuse reflectance spectra were acquired using a JASCO V-670 spectrophotometer. The particle morphology was examined by field-emission scanning electron microscopy (FE-SEM; Hitachi, S-4700). Transmission electron microscopy (TEM) images and selected area electron diffraction (SAED) patterns were acquired using a field-emission transmission electron microscope (JEOL, JEM-2800). Elemental analysis was performed using inductively coupled plasma atomic emission spectroscopy (ICP-AES; Shimadzu, ICPS-8100), X-ray fluorescence (XRF; Shimadzu, EDX-800HS), and oxygen/nitrogen combustion analysis (Horiba, EMGA-620W/C).

3. Results and discussion

Fig. 1 shows XRD patterns for $BaNbO_2N$ particles before and after flux treatment using the different alkali chlorides. Before the flux treatment, almost all diffraction peaks were assigned to $BaNbO_2N$ (PDF 01-084-1749), with a trace amount of $BaNbO_x$ being present. Following the flux treatment, although the dominant diffraction peaks were still associated with $BaNbO_2N$, some other phases, such as NbO_xN_y, were also observed (see Fig. S1 in ESI†). Except for the case of $BaNbO_2N$(LiCl), the $BaNbO_2N$ peak intensities increased following the flux treatment, and the full width at half maximum (FWHM) of the (110) peak decreased. This indicates that the crystallinity of the $BaNbO_2N$ particles was improved. As shown in Fig. S2,† the (220) peak position shifted to a slightly higher angle in the case of $BaNbO_2N$(NaCl), and to a slightly lower angle for $BaNbO_2N$(CsCl). Since the ionic radius of Ba^{2+}, Na^+, K^+, Rb^+, and Cs^+ is 0.16, 0.14, 0.16, 0.17, and 0.18 nm (coordination number: 12), respectively, these flux cations substituted for Ba ions in the oxynitride to a certain

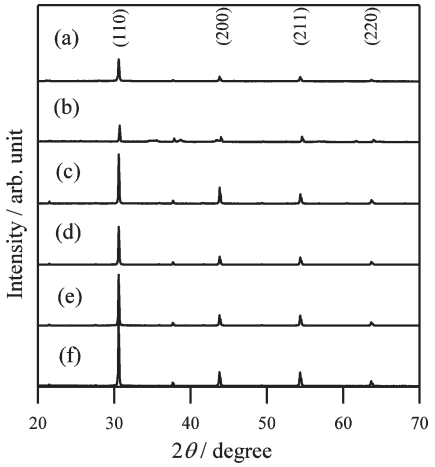

Fig. 1 XRD patterns for $BaNbO_2N$ particles (a) before and after flux treatment with (b) LiCl, (c) NaCl, (d) KCl, (e) RbCl, and (f) CsCl.

extent. Indeed, the results of the elemental analysis shown in Table S1† indicate that although the flux-treated $BaNbO_2N$ was almost stoichiometric, a few mol% of alkali metal species was present. As shown in Fig. S1,† in the case of $BaNbO_2N$(NaCl), $BaNbO_2N$(KCl), $BaNbO_2N$(RbCl), and $BaNbO_2N$(CsCl), the intensity of the XRD peaks assigned to the NbO_xN_y phase became higher following flux treatment. This suggests that a partial chemical reduction of Nb compounds had occurred.

Fig. 2 shows diffuse reflectance spectra of $BaNbO_2N$ particles before and after flux treatment. Apart from $BaNbO_2N$(LiCl), all of the flux-treated samples exhibited a clear absorption edge at about 740 nm, similar to that for untreated $BaNbO_2N$, and increased absorption was seen at longer wavelengths. The enhanced absorption at wavelengths longer than the absorption edge suggests the existence of chemically reduced Nb species or anion vacancies. However, since the elemental analysis results

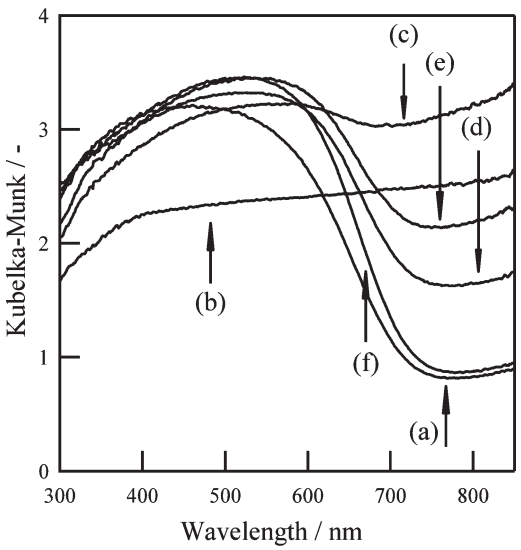

Fig. 2 Diffuse reflectance spectra of $BaNbO_2N$ particles (a) before and after flux treatment with (b) LiCl, (c) NaCl, (d) KCl, (e) RbCl, and (f) CsCl.

indicated that the flux-treated $BaNbO_2N$ was almost stoichiometric, the former explanation is more likely.

Fig. 3 shows SEM images of $BaNbO_2N$ particles before and after flux treatment. Before the flux treatment, the morphology was indeterminate, with aggregations of small particles with sizes of a few tens to a few hundreds of nanometers. After the flux treatment, a marked change in morphology occurred. For both $BaNbO_2N$(NaCl) and $BaNbO_2N$(CsCl), a cubic morphology was clearly observed. On the other hand, for $BaNbO_2N$(KCl) and $BaNbO_2N$(RbCl), most of the particles had a truncated octahedral shape. Similar flux-induced morphology changes were also reported for $SrTiO_3$.[20]

To examine the particle microstructure in more detail, TEM observations of $BaNbO_2N$(NaCl) were conducted. Fig. 4 shows a TEM image of a typical cubic particle. It is seen to contain clear grain boundaries, indicating that it is actually a secondary particle made up of primary particles with sizes of several hundred nanometers. Fig. 5(A) shows a higher magnified TEM image of the secondary particle, and Fig. 5(B) shows SAED patterns obtained for the regions indicated in Fig. 5(A) and for the entire region. All of the SAED patterns are clearly spot-like, indicating that the individual primary particles are single crystals. In addition, the similarity of the SAED pattern obtained for the entire region in Fig. 5(A) shows that all of the primary particles have the same orientation.

Next, treatments using potassium-based fluxes with different anions (KF, KCl, KBr, and KI) were performed. Fig. 6 and 7 show XRD patterns and diffuse reflectance spectra, respectively, for $BaNbO_2N$(KF), $BaNbO_2N$(KCl), $BaNbO_2N$(KBr), and $BaNbO_2N$(KI). For $BaNbO_2N$ (KF), no diffraction pattern or

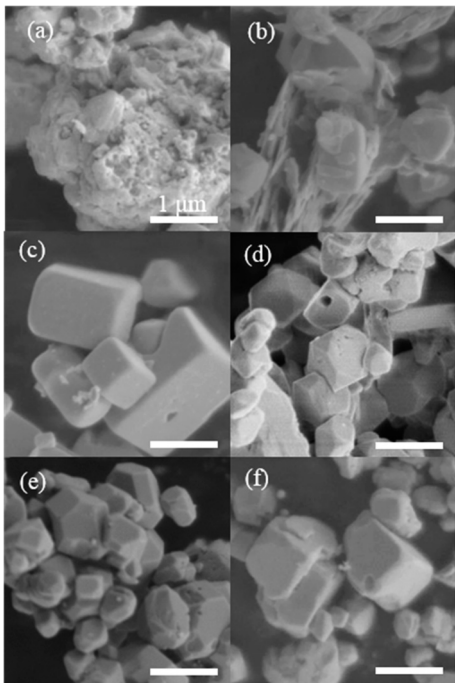

Fig. 3 SEM images of $BaNbO_2N$ particles (a) before and after flux treatment with (b) LiCl, (c) NaCl, (d) KCl, (e) RbCl, and (f) CsCl. Scale bars represent 1 μm.

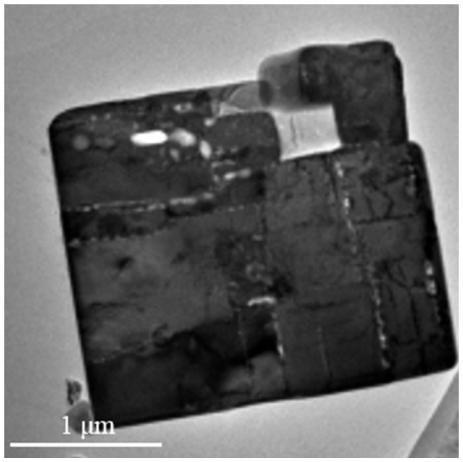

Fig. 4 TEM image of $BaNbO_2N$ particle following NaCl flux treatment.

absorption edge associated with $BaNbO_2N$ was observed, suggesting that the $BaNbO_2N$ crystal structure was not maintained after the KF flux treatment. In the case of $BaNbO_2N$(KCl), $BaNbO_2N$(KBr), and $BaNbO_2N$(KI), stronger $BaNbO_2N$ diffraction peaks were observed after the flux treatment, although peaks due to NbO_xN_y were also detected. In addition, the absorption edge at about 740 nm associated with $BaNbO_2N$ was observed, but with

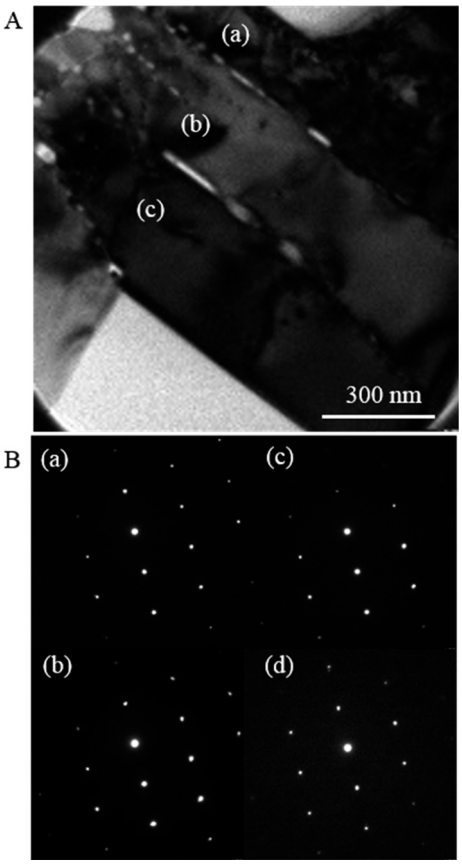

Fig. 5 (A) TEM image of $BaNbO_2N$ particle following NaCl flux treatment, and (B) SAED patterns for points indicated in (A); (d) shows SAED pattern for entire region in (A).

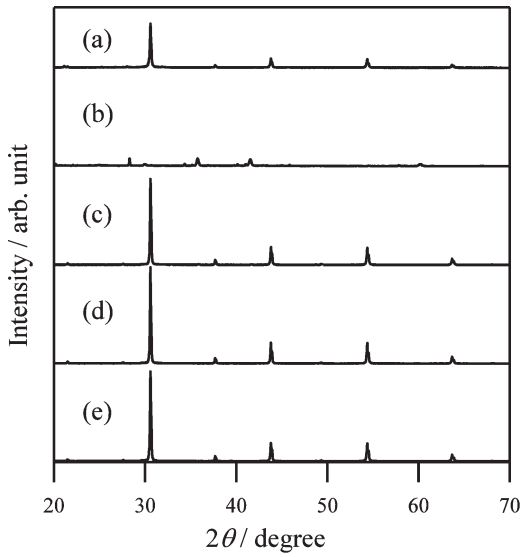

Fig. 6 XRD patterns for $BaNbO_2N$ particles (a) before and after flux treatment with (b) KF, (c) KCl, (d) KBr, and (e) KI.

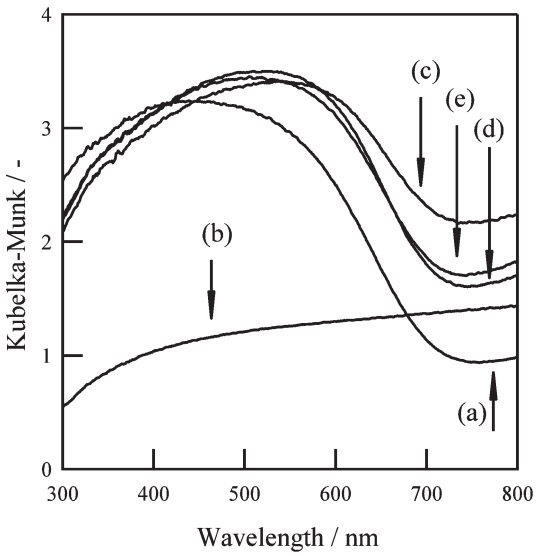

Fig. 7 Diffuse reflectance spectra of $BaNbO_2N$ particles (a) before and after flux treatment with (b) KF, (c) KCl, (d) KBr, and (e) KI.

higher absorption at longer wavelengths than for the untreated samples. As shown in Fig. 8, SEM observations revealed that all of the flux-treated samples contained particles with a similar truncated octahedral shape, except for $BaNbO_2N$(KF). These results indicate that the kind of anion in the flux did not affect the morphology of the $BaNbO_2N$ particles.

As described in the Experimental section, most of the flux evaporated during the treatment process, which was carried out a temperature that was more than 100 K higher than the flux melting point. To clarify the effects of the amount of flux on the particle morphology, flux treatment using a volatile flux flow was performed using the setup shown schematically in Fig. S3.† It consisted of two alumina boats that were placed in an alumina tube. The upstream and downstream boats

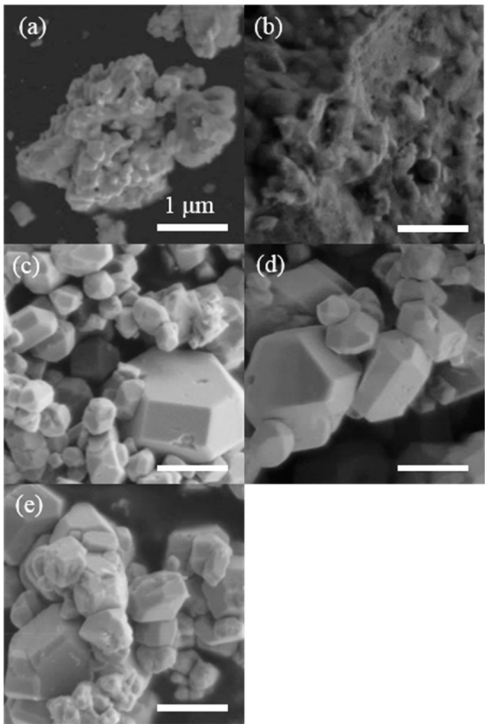

Fig. 8 SEM images of $BaNbO_2N$ particles (a) before and after flux treatment with (b) KF, (c) KCl, (d) KBr, and (e) KI. Scale bars represent 1 μm.

contained an NaCl flux and $BaNbO_2N$ particles, respectively. The molar ratio of NaCl to $BaNbO_2N$ was set to 20. During the flux treatment, the boats were heated to the same temperature. After 3 h at 1173 K under an NH_3 flow of 100 mL min^{-1}, a plentiful supply of the NaCl flux still remained in the upstream boat. Fig. 9 shows an SEM image of $BaNbO_2N$ particles after flux treatment with NaCl using this setup. It can be seen that cubic particles similar to those in Fig. 2(c) were observed. Thus, a continuous flow of vaporized flux was also effective for changing the particle morphology. A similar effect of vaporized flux has been reported for $BaTiO_3$.[21] The two-boat method used in the present study can also be applied to other synthesis systems such as a two-zone furnace,

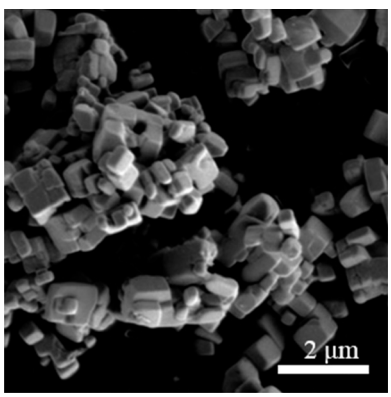

Fig. 9 SEM image of $BaNbO_2N$ particles after NaCl flux treatment using two-boat method.

and will allow more precise control of the flux, and lead to further development of the flux method.

4. Conclusions

In the present study, the effect of flux treatment using different alkali halides on $BaNbO_2N$ particles was investigated. Using NaCl or CsCl as the flux, highly crystalline cubic particles were obtained, while using KCl, KBr, KI, or RbCl, truncated octahedral shapes were observed. These results indicate that the kind of cation in the flux strongly affects the morphology of $BaNbO_2N$. The flux-treated $BaNbO_2N$ was almost stoichiometric, particularly with regard to the O/N ratio, although a few mol% of alkali metal species was present. Moreover, the results obtained using a two-boat setup showed that a vaporized flux was also effective for changing the particle morphology.

Acknowledgements

This work was supported in part by Grants-in-Aid for Specially Promoted Research (no. 23000009) and "Nanotechnology Platform" of the Ministry of Education, Culture Sports Science and Technology (MEXT), Japan. The authors would like to acknowledge Dr. Taro Yamada in the University of Tokyo for performing the ICP measurement and O/N analysis.

References

1 M. Jansen and H. P. Letschert, *Nature*, 2000, **404**, 980–982.
2 Y.-L. Kim, P. M. Woodward, K. Z. Baba-Kishi and C. W. Tai, *Chem. Mater.*, 2004, **16**, 1267–1276.
3 A. Gomathi, S. Reshma and C. N. R. Rao, *J. Solid State Chem.*, 2009, **182**, 72–76.
4 R. Marchand, Y. Laurent, J. Guyader, P. L'Haridon and P. Verdier, *J. Eur. Ceram. Soc.*, 1991, **8**, 197–213.
5 A. Kudo and Y. Miseki, *Chem. Soc. Rev.*, 2009, **38**, 253–278.
6 Y. Moriya, T. Takata and K. Domen, *Coord. Chem. Rev.*, 2013, **257**, 1957–1969.
7 K. Ueda, T. Minegishi, J. Clune, M. Nakabayashi, T. Hisatomi, H. Nishiyama, M. Katayama, N. Shibata, J. Kubota, T. Yamada and K. Domen, *J. Am. Chem. Soc.*, 2015, **137**, 2227–2230.
8 H. Urabe, T. Hisatomi, T. Minegishi, J. Kubota and K. Domen, *Faraday Discuss.*, 2014, **176**, 213–223.
9 B. Siritanaratkul, K. Maeda, T. Hisatomi and K. Domen, *ChemSusChem*, 2011, **4**, 74–78.
10 T. Hisatomi, C. Katayama, Y. Moriya, T. Minegishi, M. Katayama, H. Nishiyama, T. Yamada and K. Domen, *Energy Environ. Sci.*, 2013, **6**, 3595–3599.
11 J. W. Liu, G. Chen, Z. H. Li and Z. G. Zhang, *Int. J. Hydrogen Energy*, 2007, **32**, 2269–2272.
12 S. Feng and R. Xu, *Acc. Chem. Res.*, 2001, **34**, 239–247.
13 J. Yu and A. Kudo, *Adv. Funct. Mater.*, 2006, **16**, 2163–2169.
14 J. Boltersdorf, N. King and P. A. Maggard, *CrystEngComm*, 2015, **17**, 2225–2241.
15 Y. Mizuno, H. Wagata, K. Yubuta, N. Zettsu, S. Oishi and K. Teshima, *CrystEngComm*, 2013, **15**, 8133–8138.
16 M. Hojamberdiev, A. Yamaguchi, K. Yubuta, S. Oishi and K. Teshima, *Inorg. Chem.*, 2015, **54**, 3237–3244.
17 T. Takata, D. Lu and K. Domen, *Cryst. Growth Des.*, 2010, **11**, 33–38.
18 Y.-I. Kim, *Ceram. Interfaces*, 2014, **40**, 5275–5281.
19 T. Hisatomi, C. Katayama, K. Teramura, T. Takata, Y. Moriya, T. Minegishi, M. Katayama, H. Nishiyama, T. Yamada and K. Domen, *ChemSusChem*, 2014, **7**, 2016–2021.
20 H. Kato, M. Kobayashi, M. Hara and M. Kakihana, *Catal. Sci. Technol.*, 2013, **3**, 1733–1738.
21 P. M. Rørvik, T. Lyngdal, R. Sæterli, A. T. van Helvoort, R. Holmestad, T. Grande and M.-A. Einarsrud, *Inorg. Chem.*, 2008, **47**, 3173–3181.

